Journal of Hydrology: Regional Studies 34 (2021) 100793

Contents lists available at ScienceDirect

Journal of Hydrology: Regional Studies

journal homepage: www.elsevier.com/locate/ejrh

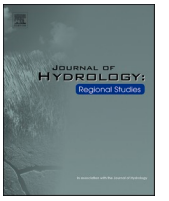

Thermal anomaly and water origin in Weebubbie Cave, Nullarbor Karst Plain, Australia

Peter Buzzacott [a], Grzegorz Skrzypek [b,*]

[a] Curtin University, Bentley, WA, Australia
[b] West Australian Biogeochemistry Centre, School of Biological Sciences, The University of Western Australia, Crawley, WA, Australia

ARTICLE INFO

Keywords:
Subterranean ecosystem
Water temperature
Stable isotopes
Flooded cave
Western Australia

ABSTRACT

Study region: The Nullarbor is one of the largest contiguous karst plains in the world. Despite the absence of surface relict karst features and arid climate, the subterranean flooded cave systems are among the largest in the world. The cave waters are usually brackish and their temperatures vary over a large range (18.6–23.7 °C) suggesting potential input of warm groundwater to some of the caves. The studied Weebubbie Cave of total length ~500 m penetrates to ~140 m below ground and ~40 m below sea level.

Study focus: Temperature loggers were deployed in the water at various depths and distances from the entry lake to detect potential warm water inputs in three different years. The stable hydrogen, oxygen, and carbon isotope compositions of water have been analysed to detect potential hydrochemical differences in inflowing water and to investigate the origin of the cave water.

New hydrological insights for the region: The thermal irregularity at the Air Dome of Weebubbie with water temperatures 0.9 °C higher than in all other cave sections, confirms some heat transfer or an inflow of warmer water. The stable isotope results suggest the cave water originates from partially evaporated (up to <20 %) modern infrequent large precipitation events. Despite the relatively high salinity (23.3 mS cm^{-1}) of the cave water, water hydrochemistry and stable isotope composition suggest that direct large ocean water contribution to the cave is unlikely.

1. Introduction

Flooded subterranean caves in remote arid regions lacking surface water provide a great window to access groundwater, allowing various studies. These caves frequently host unique ecosystems (Contos et al., 2001; Gibson et al., 2019; Tetu et al., 2013), are prone to fast pollution dispersal in the karst environment (Emmett and Telfer, 1994; Williams et al., 2014) and are vulnerable to climate change (Talà et al., 2021). They are, therefore, subject to conservation efforts (Boulton et al., 2003; Lewis, 2019; White et al., 2020). To understand and manage these subterranean ecosystems, a thorough understanding of water origin, recharge rates, nutrients budget, and water physical parameters, especially temperature, is required. However, sampling fully underwater sections of caves is extremely difficult and requires highly specialised diving skills. Therefore, compared with marine caves, flooded subterranean caves are rarely comprehensively studied, as evidenced by the relative dearth of published research describing these environments. Underwater investigations by cave divers have great potential to provide insight into ecological, speleogenetic, and hydrogeological processes, by gathering information largely unavailable to non-diving karst scientists.

* Corresponding author at: The University of Western Australia, MO90, 35 Stirling Highway, Crawley, WA, 6009, Australia.
E-mail address: grzegorz.skrzypek@uwa.edu.au (G. Skrzypek).

https://doi.org/10.1016/j.ejrh.2021.100793
Received 5 September 2020; Received in revised form 4 February 2021; Accepted 12 February 2021
Available online 24 February 2021

Arid and semi-arid zones are bounded by the latitudes of 10°–35°, poleward of the Inter-Tropical Convergence Zone. Though not all land between these latitudes is arid or semi-arid, arid or semi-arid land covers about one-third of the world's total land surface area (McKnight and Hess, 2000). Many caves are located in these zones in the karst regions of Central Spain, North Africa, Arabian Peninsula, Israel, Iran, Western China, Southwestern USA, Namibia, Chile, Mexico, and Australia. However, only a limited number of them are separated from surface ecosystems and filled with groundwater not associated with direct inflow from surface features such as rivers, streams, lakes, or oceans (Webb and White, 2013). In caves in regions lacking surface water, groundwater is replenished by diffuse recharge influenced by local factors; climate, geology, soil thickness, vegetation, geomorphology, and especially preferential flow paths (Markowska et al., 2016). Therefore, despite several common features reflecting regional conditions, each flooded cave region is unique and the caves in these zones allow direct access to their groundwater environment that would otherwise be accessible only through bores. The most common characteristics of water in these flooded caves, and groundwater in general in arid climates, are warm temperatures, elevated salinity, relatively old age, and episodically infrequent recharge (Gee and Hillel, 1988; Herczeg and Leaney, 2011). These features make caves in arid regions significantly different from more frequently studied caves in wetter and colder climates, where cave water is usually fresh and cold, frequently remaining in equilibrium with precipitation (Schwarz et al., 2009), and is constantly replenished by rivers with underground sections (Calligaris et al., 2018) or by direct seepage of river water (Vysoká et al., 2019).

Australia's largest flooded subterranean caves are located at the southern end of the Nullarbor limestone plain in Western Australia (James et al., 2012). These cave systems are unique in the world and rare in scale, with some to the extent of 36 km of mostly dry passage, up to 6.5 km of flooded passage, and up to ~50 m water depth (J. Bicanic, personal communication, 3rd September 2020) (Bicanic, 2017; Webb and James, 2006). The Nullarbor is a flat plain with relief less than 10 m, surface water is absent and there are no defined river channels that could supply the cave system. Sheetwash erosion processes occur only during flooding initiated by infrequent intense rainfall events, and during these unpredictable events runoff or flows are extremely difficult to quantify (Gillieson and Spate, 1992). Although plausible hypotheses exist, speleogenesis of the Nullarbor caves remains largely undescribed. Current hypotheses suggest that rainfall saturated with biogenic carbon dioxide from the monsoonal woodland during the relatively warm and wet Oligocene (34−23 Ma) infiltrated and dissolved shallow phreatic passages along tectonic and lithological discontinuities. Bedding interfaces and fractures were preferentially enlarged, leading to the formation of larger passages and eventually feeding springs along the coastal cliffs. Then, during the late Oligocene, rising seawater replaced freshwater in these passages slowing their karstic processes, erosion, and further cavity development (Webb and James, 2006). One main hypothesis is that these large conduit passages were then buried by roof collapse during the uplift of the Nullarbor karst during the Late Miocene when seawater hydrostatic support was withdrawn, aided thereafter by gypsum and halite crystal wedging (Gillieson and Spate, 1992; Webb and James, 2006). Since the mid-Miocene, the Nullarbor has experienced primarily an arid to semi-arid climate except for a relatively brief Pliocene wet phase 5−3 Ma (Gregoric et al., 2014). During the arid/semi-arid phases, the region was geologically and hydrologically stable, as evidenced by high retention of the original sedimentary rock substrate and lack of river flow in the south (Gregoric et al., 2014; Richards, 1971; Webb and James, 2006). Therefore, Nullarbor Plain is very flat, and relict karst surfaces are absent (Gillieson and Spate, 1992). Given the lack of watercourse relief and limited identification of apparently phreatic features within diveable Nullarbor caves, the precise character of any water flow along the gentle coastward gradient remains unidentified. Limited groundwater resources and high salinity has historically limited investment into groundwater research in the region. Therefore, little is known about Nullarbor hydrogeology and hydrochemistry (Australian Water Resources Assessment 2012 - South Western Platea).

Flooded Nullarbor caves that are of sufficient size and depth to be diveable developed in three limestone units with Nullarbor Limestone at the surface, Abrakurrie Limestone below that, and Willson Bluff Limestone the deepest; the majority of caverns developed in the latter (Webb and James, 2006). Large sections of these caves are below the groundwater table (10 m a.s.l. to 40 m b.s.l.). Therefore, groundwater likely plays a major role in the current formation of subterranean caves in the Nullarbor Plain, by eroding karst along conduits of least resistance. Moreover, water temperature is a significant factor in water density, viscosity, mineral solubility and, in consequence, water hydrochemistry (Kaufmann et al., 2014). Significant differences between cave water temperatures (18.6–23.7 °C) have been recorded across the Nullarbor Plain. In addition, long-term temporal changes in water temperature were suggested as a response to seismic activity (Buzzacott, 2011a) and may suggest some thermal water inputs or heat transfer from below the Nullarbor Plain. Therefore, this study aimed (1) to characterise spatially and temporally the water temperature in one of the Nullarbor caves, Weebubbie Cave N2, and (2) to attempt verification of the cave water origin using stable isotope methods. The results were compared with other large caves in the region (Murra El Elevyn, Cocklebiddy, and Tommy Graham's caves).

2. Materials and methods

2.1. Study site description

The Nullarbor is the largest contiguous karst plain in Australia (~200,000 km^2) and one of the largest in the world (Lowry and Jennings, 1974; Richards, 1971). It is a vast flat plateau of ~100 m thick Nullarbor Limestone Formation uniformly falling with a very low gradient (0.00005) towards the coast of the Southern Ocean (Gillieson and Spate, 1992; Richards, 1971). The surface is covered by sparse, low, arid shrub characterised by an absence of trees (from the Latin name "Null - Arbor") (Gillieson and Spate, 1992), punctuated by ephemeral carpets of grass following seasonal downpours (Lowry and Jennings, 1974). The climate is arid, with annual rainfall generally highest near the coast, 275 mm at Eucla (www.bom.gov.au, site 011003, period 1930–2010) (Bureau of Meteorology, 2013; Gillieson and Spate, 1992), influencing the ambient temperature inside caves (Gregoric et al., 2014).

More than 5,000 Nullarbor karst features have been recorded by the Cave Exploration Group of South Australia (CEGSA) and yet

less than twenty are known as both reaching the water table and of size large enough to be diveable using Self-Contained Underwater Breathing Apparatus (SCUBA). Except for two shallow systems on the low coastal Roe Plain, most of these large rare topographic features are characterised by steep-sided collapse dolines, and the youngest and most active of which are to the west side of the region. One of these features is Weebubbie Cave (N2) (Fig. 1) with a total length of ~500 m, down to ~140 m below ground level, and ~40 m below sea-level, with sections >250 m length underwater up to ~50 m deep. The Weebubbie Cave entrance is characterised by a huge 50 × 30 m collapse doline and 200 m of talus through approximately 20 m × 20 m passage to a 200 m × 10 m Main Lake dropping to 30 m depth along its sides. There is almost unrestricted heat exchange between the cave chamber, Main Lake at the cave entrance and the atmosphere outside, (Fig. 2), due to the daily circulation of large air mass as the ambient air pressure rises and falls (Bureau of Meteorology, 2013). Divers can enter the dry section of the cave heading west, and then head south across the large Main Lake until the surface of the lake (Figs. 1C and 2) is met by the cave roof. From there they can descend and either turn south-west through the Main Sump and pass beneath the Air Dome or head south through the Railway Tunnel (Figs. 1C and 2), a large relatively uniform passage reaching a terminal depth of ~45–50 m (Bicanic, 2017; Lewis, 1979). The water in Weebubbie Cave is brackish (23.3 mS/cm) and alkaline with pH 7.75 (Holmes et al., 2001), making it unsuitable for either crop irrigation or watering stock. A permit to extract water was awarded in 1928 but the endeavor failed and the lease was cancelled in 1930 (Poulter, 1987). Future technological developments, for example in agriculture or engineering, may see renewed interest in utilising water from Weebubbie Cave after, e.g., desalisation.

2.2. Logger calibration

The temperature in the cave was recorded using Sensus Ultra® loggers operational to the depth of 150 m and at temperatures between -20 °C and 40 °C. The pressure resolution was 1 mbar and accuracy ±30 mbar, equivalent to ±30 cm change in depth whilst immersed in seawater. Temperature was resolved to 0.01 °C and accurate to ±0.8 °C (Wilk, 2006). The logger sampling rate was at 10 s intervals, and the loggers were automatically activated at 1111 mbar pressure, approximating the pressure at 1 m depth (Wilk, 2006). To assess the inter-logger variability before first visiting Weebubbie Cave (2011), the 15 loggers were evenly distributed along a rod suspended below a single pivot and taken to 10 m depth in 20 °C water. After one hour of immersion, the mean recorded temperatures, estimated depths, and standard deviations between loggers over 90 s (10 samples) were 20.0 °C (SD 0.18) and 10.0 m (SD 0.05), confirming inter-logger differences much lower than factory specified accuracy. Prior to the second visit to Weebubbie Cave (2012), the loggers were again suspended on a rod below a single pivot and taken to depth for inter-logger variance measurement. They were left at 6 m for 1 h to equilibrate with the water. After equilibration, the standard deviation within each logger over 90 s recording interval was 2 cm depth and <0.1 °C. The relative difference between all 14 loggers was lower than 0.1 °C. Low inter-logger variability gives a reliability measure that is appropriate for comparison between locations.

Following retrieval, each logger was downloaded to a laptop computer and stored using software supplied by the logger

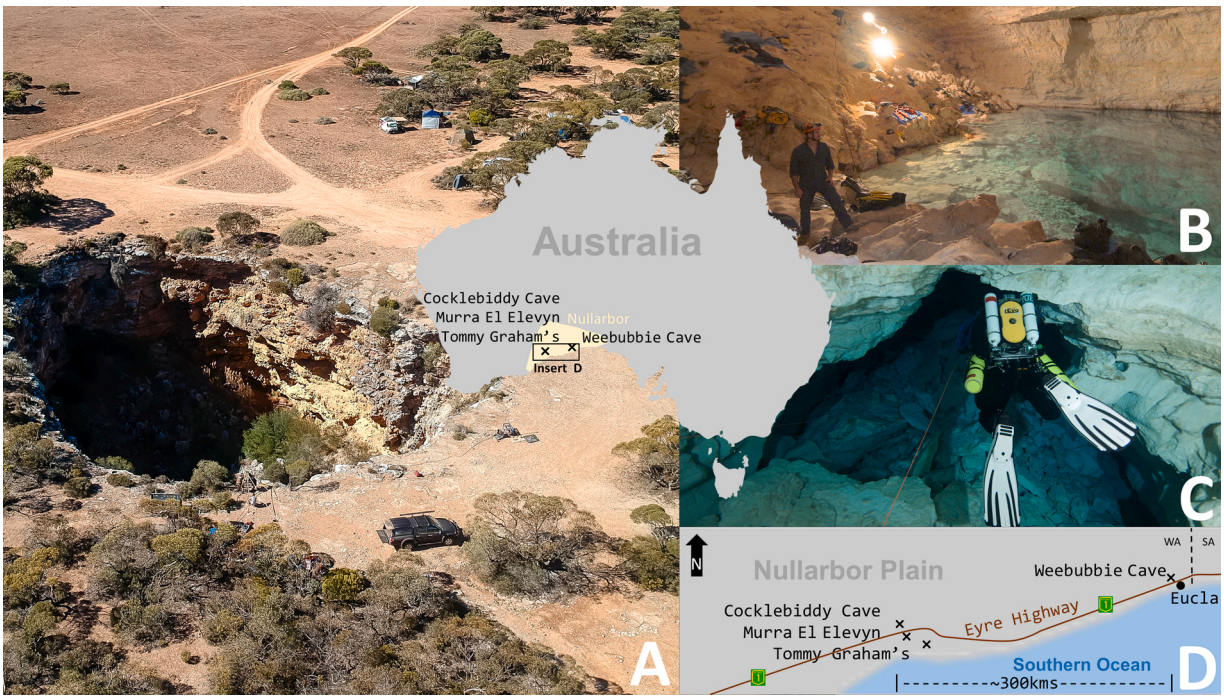

Fig. 1. Location of Weebubbie Cave (N2) in Western Australia, 31°39′13″ S and 128°46′30″ E, elevation 93 m a.s.l. (A) aerial photograph of Weebubbie Cave 2019 by S. Elliott. (B) Main Lake at the cave entry, photo by A. Fleming 2014. (C) Railway Tunnel, photo by D. Wright 2016. (D) Locations of the caves on Nullarbor Plain. Photo (A) is the sinkhole shown in Fig. 2.

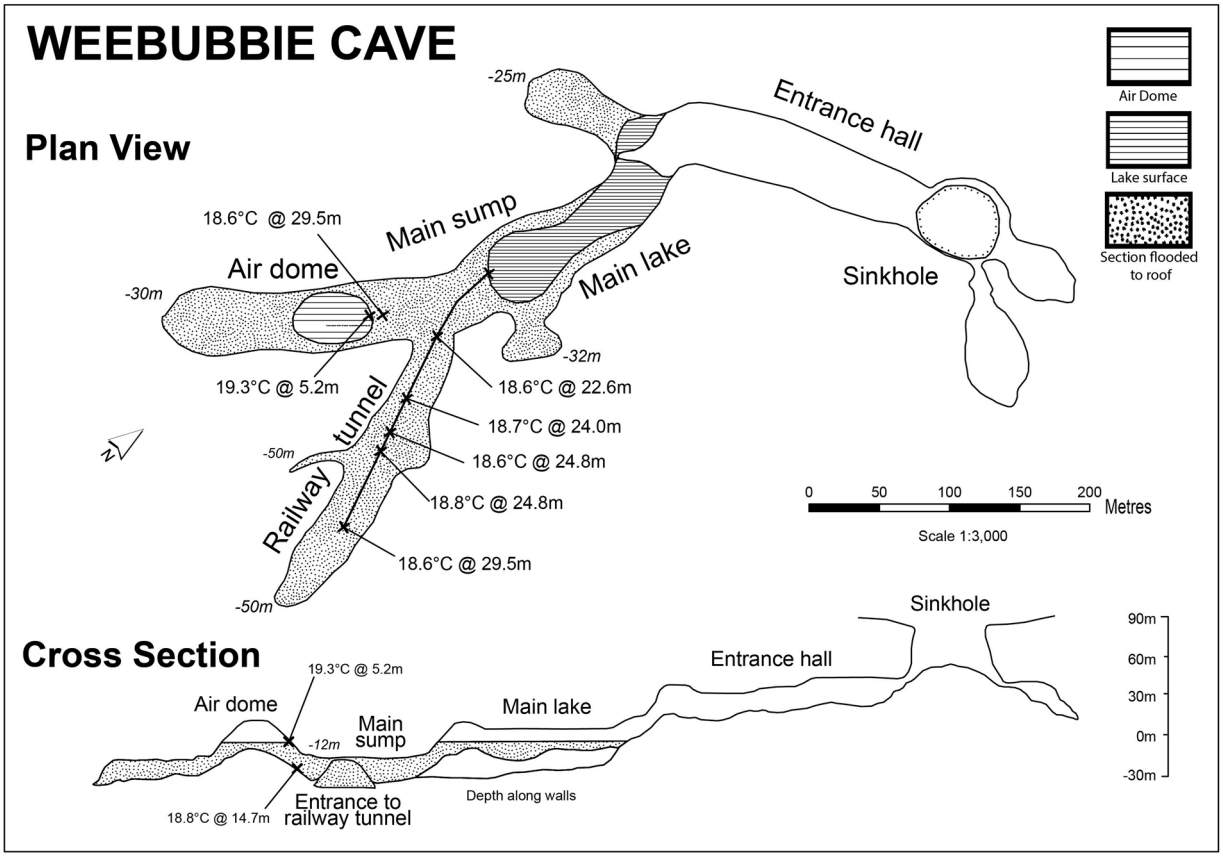

Fig. 2. The sketch of the Weebubbie Cave with mean water temperatures recorded in 2013 at given depths along the guideline across the Railway Tunnel (solid line) and the Main Sump and at the Air Dome (modified by H. Thornton after Lewis et al. 1979). The temperatures are consistent with those recorded in 2012 by the logger worn by a diver [PB] (Fig. 4 and Table 2). Photo of the cave entrance, sinkhole, is presented in Fig. 1A.

manufacturer (ReefNet, Mississauga, Canada) (Wilk, 2006). In all three visits, 10 samples of 10 s measurements were averaged from each logger reflecting 90 s mean water temperatures and depths. Means with standard deviations (in parentheses) are reported.

2.3. Temperature measurement and logger emplacement

Weebubbie Cave was studied over three visits in October 2011, November 2012, and October 2013. During the first visit (2011) loggers were attached to the guideline running from the Main Sump into the Railway Tunnel (see Fig. 2), spaced approximately every 15 m for a total length of 210 m. The loggers were left overnight and retrieved after no less than 16 h in situ.

During the second visit (2012) five of the same loggers were attached to a vertical line suspended between a float and a weight in the Main Lake, at 15 m in front of the entrance to the flooded passage. They were left in place in the Main Lake for 80 min. An additional logger was worn by one of the divers who re-visited the Main Sump swimming along the passage where a semi-permanent guideline is installed (see Fig. 2), before surfacing in the Air Dome.

A year later a third field trip (2013) was undertaken, both to measure the perceived temperature gradient underneath the Air Dome, and to collect water samples for analysis. Sensus loggers were again placed along the guideline that runs from the Main Sump through the Railway Tunnel, but this time two additional loggers were also suspended beneath a float in the Air Dome, and two loggers were suspended 0.5 m above the floor of the cave beneath the Air Dome (Fig. 2).

2.4. Collection and analyses of water for stable hydrogen, oxygen, and carbon isotope compositions

During the October 2013 trip, water samples were collected underwater from inside the Railway Tunnel at points along the nylon guideline where Sensus loggers were also placed (Fig. 2), from the Air Dome, and from near the floor directly below it. Prior to the dive each 40 mL glass vial (Chromacol, Thermo Scientific, USA) was filled with water from the Entry Lake to prevent them from breaking due to pressure differences. At the underwater sampling points, each vial was flushed three times using a 50 mL syringe with tubing to reach the vial bottom and capped. Sealed vials were kept in an electric refrigerator (Engel Distribution Pty Ltd, Perth, Australia) set to a few degrees Celsius above freezing during transportation to West Australian Geochemistry Centre at The University of Western

Australia. In addition, for comparison with Weebubbie Cave, water samples for stable isotope analyses were also collected from Cocklebiddy cave in January 2012, and from two other caves in October 2013: Tommy Graham's and Murra-El-Elevyn. Rainwater monthly samples have been collected at Maryland Loo (33.47 °S 121.07 °E) sampling station maintained by The University of Western Australia using the precipitation sampler recommended by International Atomic Energy Agency (Gröning et al., 2012).

The stable isotope composition of water samples was analysed using an Isotopic Liquid Water Analyser Picarro L1115-i (Picarro, Santa Clara, California, USA). Each sample was analysed six times and then the first four results were discarded to minimize any instrument memory effect (Van Geldern and Barth, 2012). The δ^2H and δ^{18}O values of samples were normalized to the VSMOW2-SLAP2 international scale based on three laboratory standards. Each standard was replicated twice and the results were reported in per mil (‰) following the principles of the three-point normalization (Skrzypek, 2013). All laboratory standards were calibrated against primary international reference materials that determine the VSMOW2-SLAP2 scale (Coplen, 1996), provided by the International Atomic Energy Agency (for VSMOW2 δ^2H and δ^{18}O of equal 0 ‰ and for SLAP equal δ^2H = −428.0 ‰ and δ^{18}O = −55.50 ‰). The long-term analytical uncertainty (one standard deviation) was determined as <1.0 ‰ for δ^2H and <0.10 ‰ for δ^{18}O (Skrzypek and Ford, 2014).

The stable carbon isotope composition of dissolved inorganic carbon (DIC) was analysed using GasBench II coupled with Delta XL Isotope Ratio Mass Spectrometer (Thermo-Fisher Scientific, Bremen, Germany) (Paul and Skrzypek, 2007). All results were expressed using the standard δ-notation (δ^{13}C) and were reported in per mil (‰) and normalised to Vienna Pee Dee Belemnite isotope scale (VPDB). The multi-point normalization was based on three international standards NBS18, NBS19, and L-SVEC each replicated twice (Skrzypek, 2013). The analytical uncertainty was <0.10 ‰ (one standard deviation).

2.5. Statistical analysis

Normality was assessed using SAS (Statistical Analysis Software ver 9.1, Cary, NC) PROC UNIVARIATE, and the Wilcoxon Rank-Sum test was used to assess the homoscedasticity of the data set (PROC NPAR1WAY). A general linear model (PROC GLM) was used to assess the relationships between temperature, depth, distance, and trip (Eq. 1):

$$\text{Temperature} = \alpha + \beta_1\text{Depth} + \beta_2\text{Distance} + \beta_3\text{Trip} \quad (1)$$

where α is the intercept and $\beta_{1\text{-}3}$ are the parameter estimates for the respective independent variables.

In addition, samples of ten data recorded by the logger worn by the diver in the second trip (2012) in the Entry Lake, the Main Sump, ascending and descending in the Air Dome and back in the Entry Lake were each pairwise tested for a significant difference to the samples recorded by the static loggers in the Railway Tunnel (during 2011 and 2013), again using a general linear model (PROC GLM).

Local Water Meteoric Line (LMWL) was calculated using monthly precipitation and following the recommendation of International Atomic Energy Agency (Fig. 5) (Gröning, 2011). LMWL was calculated using a precipitation amount weighted least squares regression method (PWLSR) that correct biases caused by more frequent low precipitation events strongly affected by below cloud evaporation (Hughes and Crawford, 2012). Local Evaporation Line (LEL) and mixing lines (Fig. 5) were calculated using an ordinary least squares regression (OLSR), which gives equal weighting to all data points.

3. Results

Mean water temperature recorded by the static loggers installed in Weebubbie Cave from the Main Sump across the Railway Tunnel were not significantly different between the three different years (2011, 2012, and 2013) and varied between 18.6 and 18.7 °C (Table 1). The maximum difference between the minimum and maximum from the Main Sump and throughout the Railway Tunnel (210 m length) and the water column (29.5 m depth) during each year was within a 0.5 °C range (SD 0.1 °C) (Fig. 3).

Water temperature recorded by static loggers during the first two field trips (2011 and 2012) was not significantly correlated with either trip year ($p = 0.58$) or with distance into the cave ($p = 0.96$) but was significantly correlated with depth ($p = 0.01$). However, the temperature change with depth was small, decreasing by 0.05 °C for every increase in depth of 10 m (Fig. 3, Tab S1 Supplementary Materials). Therefore, in practical terms, the water from the Main Sump into the Railway Tunnel may be considered homogenous regardless of depth or distance from the cave entrance lake.

Table 1
Water temperature in Weebubbie Cave from the Main Sump through the Railway Tunnel (total studied length 210 m) recorded using static loggers.

Field Trip	Mean Temperature [°C]	Range (difference) [°C]	Standard Deviation [°C]
October 2011 (n = 140) horizontal line 210 m	18.6	18.3–18.8 (0.5)	0.1
November 2012 (n = 50) vertical line ~5–20 m	18.6	18.5–18.7 (0.2)	0.1
October 2013 (n = 50) horizontal line 210 m	18.7	18.6–18.8 (0.2)	0.1
Overall (n = 240)	18.6	18.3–18.8 (0.5)	0.1

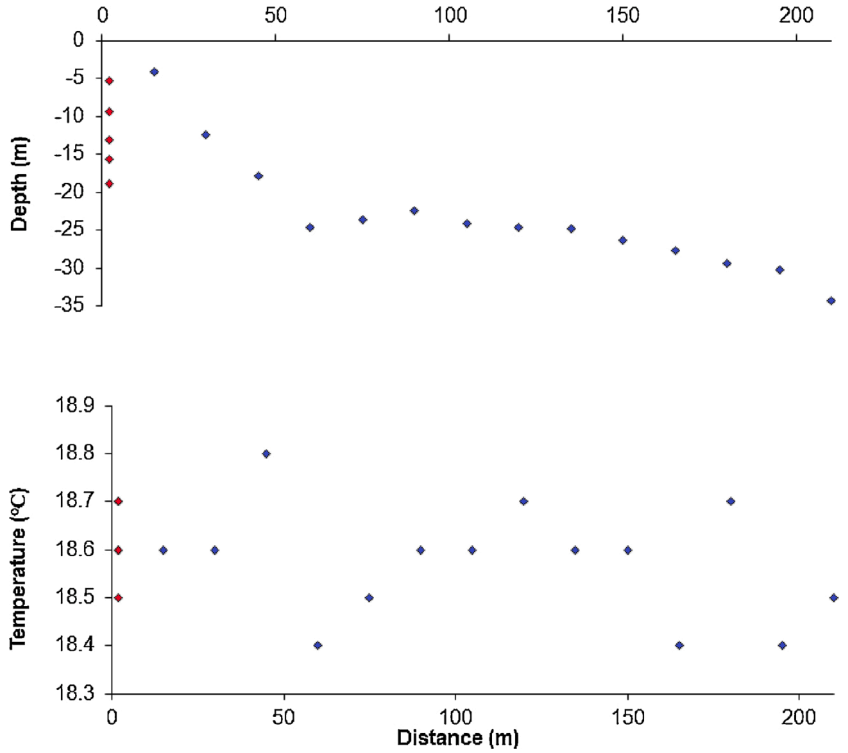

Fig. 3. Water temperature in Weebubbie Cave from the Main Sump through the Railway Tunnel recorded using static loggers in October 2011 (blue). Logger depths and temperatures at distance = 0 m (within the entry lake) recorded November 2012 (note, three temperatures of 18.6 °C plotted on top of each other, red). Temperature measurement inter-logger variability is ±0.18 °C.

Contrastingly, higher temperatures were detected in 2012 during temperature mobile measurements in the passage leading to the Air Dome. Two divers entered the Main Sump, passed underneath the rock arch at 12 m depth, and ascended to the Air Dome (Fig. 2). The divers remained in the Air Dome for 20 min before exiting via the same route directly under the arch at the depth of 12 m. Warmer water was recorded by the logger worn by one of the divers [the author PB] from the depth of 7.6 m to the surface in the Air Dome (depth displayed by Dive Computer, VR3 Technology Limited, Poole, UK). The 10 temperature data points recorded during the ascent and descent into and from the Air Dome (Fig. 4) were significantly higher than recorded elsewhere in the cave ($p < 0.001$), with a maximum recorded temperature of 19.5 °C (Table 2). Though not left in situ long enough to equalise, the water temperature recorded by the logger worn by the diver back in the Main Lake while retrieving the static loggers was commensurate with the mean water temperature recorded by them (18.8 °C vs. 18.6 °C).This confirmed the validity of the recording of relatively warmer water in the Air Dome (Table 2).

The temperature data recorded by the logger worn by the diver in 2012 was confirmed by two static loggers installed at the Air Dome in 2013. Mean recorded water temperatures (mean of 10 consecutive samples recorded at 10 s intervals) were lower at 18.8 °C (SD 0.00) below the air dome at depth 14.7 m (SD 0.00) and higher at 19.3 °C (SD 0.01) near the Air Dome at depth 5.2 m (SD 0.00) (Fig. 2).

The stable hydrogen and oxygen isotope composition of water (δ^2H and δ^{18}O) were highly homogeneous and the difference between the Main Sump, the Air Dome, and the Railway Tunnel was insignificant. All results for δ^2H and δ^{18}O varied in the range expected for the analytical uncertainty with an average of -31.1 ± 1.2 ‰ and −4.34 ± 0.05 ‰, respectively (Fig. 5). Also, the stable carbon isotope composition of dissolved inorganic carbon was highly homogenous with an average δ^{13}C(DIC) of 0.4 ± 0.1 ‰.

4. Discussion

4.1. Temperature of cave water

Cave air and water temperatures vary with respect to multiple factors, including local mean air temperature above the ground, seasonal changes in flooding or infiltrating water volume and temperature, cave depth, geothermal gradient, geomorphology, and cave-to-atmosphere heat exchange (Lachniet, 2009; Rau et al., 2015; Zhang et al., 2008). In many caves, the air temperature reflects the long-term mean air temperature and groundwater temperature largely reflects the temperature of the season contributing the most to the groundwater recharge (Jasechko et al., 2017; Rau et al., 2015). Therefore, caves located in the same region are characterised usually by similar temperatures. However, in Nullarbor caves located within a 15 km radius, there was considerable variation in water

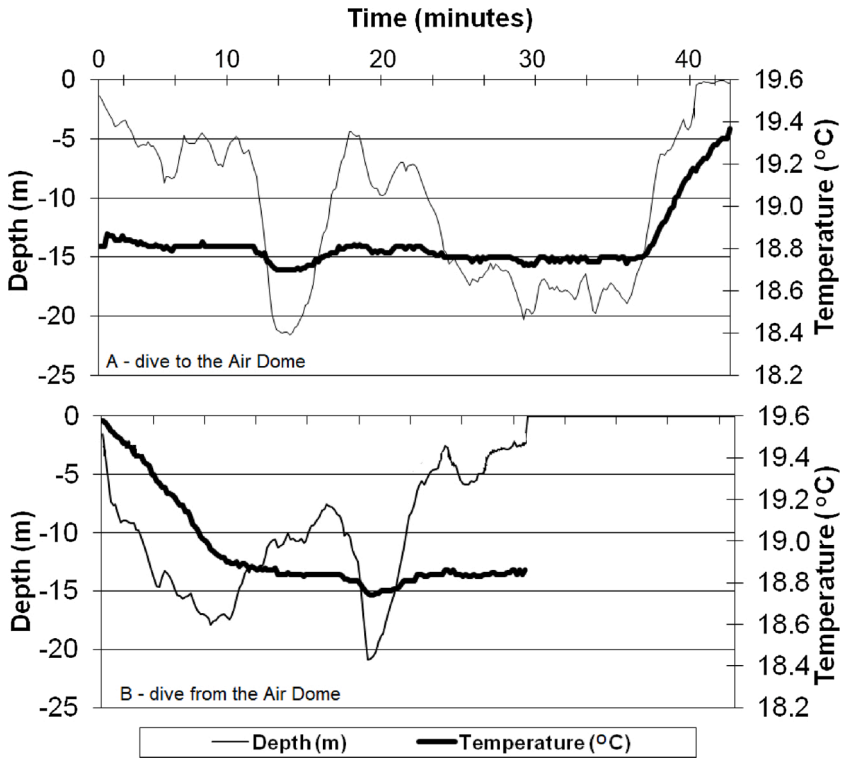

Fig. 4. Temperature and depth were recorded by the logger worn by the diver during the dive to (A) and from (B) the Air Dome October 2012. These results are consistent with static loggers suspended in the passage to the Air Dome in 2013 (Fig. 2). Temperature measurement precision is ±0.10 °C.

temperatures (Cocklebiddy 19.5 °C, Tommy Graham's 23.4 °C, Murra-El-Elevyn 18.9 °C in 2009) (Buzzacott, 2011a, b; Contos et al., 2001; Holmes et al., 2001). Moreover, seismic activities (the last local earthquake was in 1992) have been hypothesised as a reason for water temperature long–term trends, leading to a decrease of the cave water temperature by 4.8 °C in Murra-El-Elevyn between 1999 and 2009 (Buzzacott, 2011a).

The water temperature of 18.9 °C (22 m depth) reported earlier (Contos et al., 2001) for Weebubbie Cave in either 1999 or 2000 (although the sampling methodology remains undescribed) is consistent with temperatures recorded during this study. Mean water temperature (18.6 °C, SD 0.1) in the Main Sump and the Railway Tunnel was consistent over three years (2011, 2012, 2013) and uniform over the length of 210 m with the maximum spatial difference of 0.5 °C (Figs. 2 and 3). However, during the second field trip in 2012, a warm 'pool' of water at 19.5 °C was confirmed at the Air Dome, with temperatures 0.9 °C higher than in the Main sump and the Railway Tunnel (Fig. 4). This statistically significant difference was confirmed in 2013 by installing static loggers in the passage leading to the Air Dome (Fig. 2). Given that the only observable way for water to flow into and out of the Air Dome would be underneath an arch at 12 m depth, it appears that warmer water entering the cave is being trapped in the passage leading to the Air Dome. If this is a stable phenomenon, then the heat capacity of this water, determined by its temperature-volume relationship, must be sufficient to maintain the water at this elevated temperature, assisted by relatively low atmospheric exposure within the Air Dome (surface area ~300 m^2). Though the source of the warmer water in the Air Dome has not yet been identified, the possibility must be considered that warm water is entering the cave or heat is transferred to the cave through the floor or walls and rising into the Air Dome, where it is trapped by the rock arch at 12 m. Another possibility could be that warmer water may be entering Weebubbie Cave at other, as yet unidentified, locations and while mixing with the ambient water move towards the passage to the Air Dome. The Air Dome chamber is located ~90−100 m below the ground surface and it is unknown at this stage if it has direct contact with the atmosphere through cracks or an unidentified blowhole, allowing movement of air between the cave and the atmosphere due to daily pressure changes. Also, the direction the water flows in the cave has not been studied yet.

The mean cave water temperature (18.6 °C) is commensurate with the mean annual air temperature recorded at Eucla weather station (www.bom.gov.au, site 011003, period 1930–2010) of 19.0 °C mean at 9.00 AM and 19.7 °C mean at 3.00 PM. Slightly lower temperatures of cave water, compared to mean air temperature, can be explained by higher contribution from precipitation occurring during the cold season April to August (60 % of precipitation) to the groundwater recharge. The similarity between groundwater temperature and the mean annual air temperature is a typical phenomenon observed world-wide and ambient cave temperature is within the range expected for local groundwater (Jasechko et al., 2017). However, as suggested above, higher temperatures at the Air Dome (19.5 °C) may suggest some local input of warmer water or heat transfer without the physical input of water to the cave. To investigate a possible local source of warmer water we analysed the stable isotope composition of water and dissolved inorganic

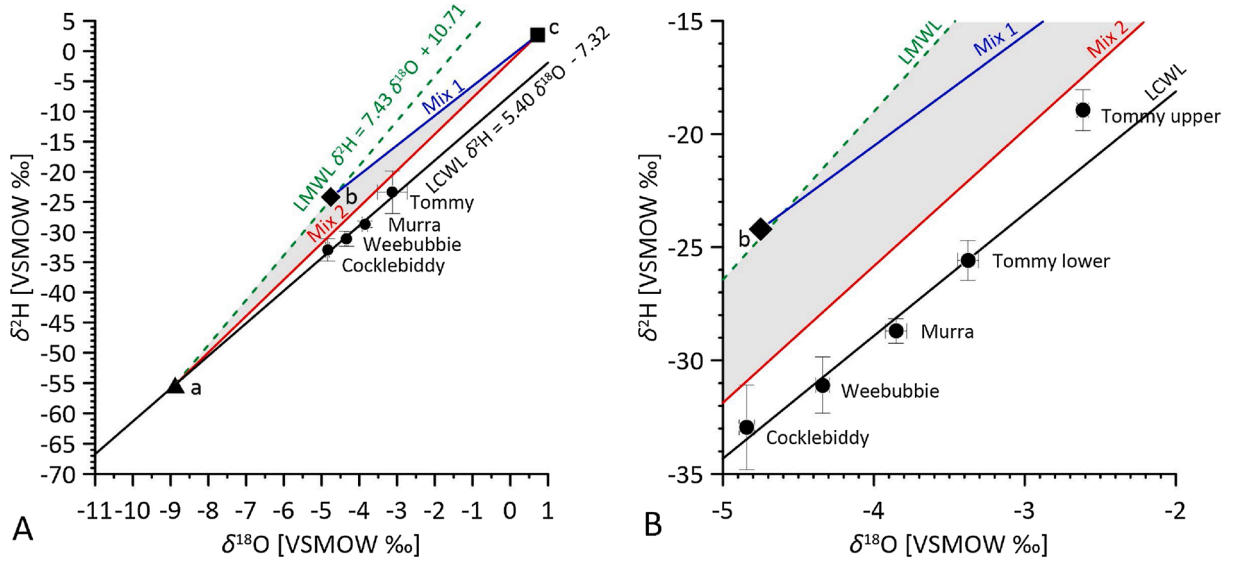

Fig. 5. (**A**) Stable hydrogen and oxygen isotope compositions of Weebubbie Cave water in comparison to other caves in the region and Local Meteoric Water Line (LMWL-PWLRS) for the nearest precipitation sampling station (Maryland Loo, 33.47 °S 121.07 °E). Error bars reflect variability in the cave given as one standard deviation. The diamond symbol (b) represents weighed by volume mean rainfall (δ^{18}O −4.75 ‰, δ^{2}H −24.2 ‰, 12 mths mean at Maryland Loo). Mix 1 represents a hypothetical mixing line between the local ocean water (δ^{18}O 0.72 ‰ and δ^{2}H 2.63 ‰) (square symbol c) and the mean rainfall (diamond symbol b). Mix 2 represents a hypothetical mixing line between the local ocean water (c) and large volume precipitation represented by the crossing point (triangle symbol a) between LMWL and LCWL, δ^{18}O −8.88 ‰ and δ^{2}H −55.3 ‰. The grey areas represent mixing polygon between three end-members and the hypothetical range of values for cave water if these three end-members would be contributing. (**B**) Zoomed in plot area (A) with the results for cave water, Tommy Graham's Cave water represented by two points for upper and lower water masses.

Table 2
Data recorded by the logger worn by a cave diver [author, PB] in October 2012.

Location (chronological order) (n = 10 for each)	Mean depth [m] (SD)	Mean Temperature [°C] (SD)	Difference to Main Sump[†] [°C]
Placing the static loggers	21.2 (0.3)	18.7 (0.0)	0.1
The Railway Tunnel	18.0 (0.3)	18.7 (0.0)	0.1
Ascent into the Air Dome	0.2 (0.1)	**19.3 (0.0)**	**0.7**[§]
Descent from the Air Dome	6.8 (2.6)	**19.5 (0.0)**	**0.9**[§]
Retrieving the static loggers	19.3 (1.4)	18.8 (0.0)	0.2

Bold indicates physically detected by the diver wearing the instrument.
[†] After adjustment for the effect of depth.
[§] $p < 0.001$.

carbon.

4.2. Stable hydrogen and oxygen isotope composition of cave water

The stable hydrogen and oxygen isotope composition of water in the Weebubbie Cave Main Sump and the Railway Tunnel (δ^{18}O −4.34 ± 0.09 ‰ and δ^{2}H −31.1 ± 2.2 ‰) is highly homogenous and not different from the water composition in the passage leading to the Air Dome, where the thermal anomaly was observed (Table S1, Fig. 2). This lack of detectable differences suggests heat transfer rather than the physical inflow of warm water. If the inflow of warm water at the Air Dome is present, then the inflowing warm water would have to have a stable isotope composition very similar to water in other parts of the cave. The direct inflow cannot be excluded at this stage of the study; however, geothermal water often has different hydrochemistry and stable isotope composition, especially if it is associated with deep circulation (Awaleh et al., 2020; Burnside et al., 2016; Fusari et al., 2017). Therefore, heat transfer is inferred.

The origin of water in the cave and potential contributions from different sources were verified using the stable isotope composition and linear regression models. The position of the cave water δ-values was analysed in relation to Local Meteoric Water Line (LMWL) and mixing lines for potential end-members (Fig. 5AB). Three end-members potentially contributing to the cave water were considered: 1) weighed by volume local mean annual precipitation, 2) high volume precipitation events only, and 3) ocean water.

The stable isotope composition of weighted by volume annual mean local precipitation ($\delta^{18}O$ −4.51 ‰ and $\delta^{2}H$ −23.5 ‰) was initially calculated for the geographic coordinates and altitude of Weebubbie Cave using the Online Isotopes in Precipitation Calculator (Bowen and Revenaugh, 2003) and based on long-term observation from Australian Global Network of Isotopes in Precipitation stations (GNIP/IAEA). However, the closest GNIP stations are very far from the cave: Adelaide 1,100 km to the east, Alice Springs 1, 000 km to the north, and Perth about 1,200 km to the west. Considering large distances between the GNIP stations and the cave, likely considerably contributing to uncertainty in interpolation, more local results from the same coast but from shorter time series were obtained (May 2015-April 2016, Table S2). The weighted by volume annual means, as directly observed at Maryland Loo near Esperance (33.47 °S 121.07 °E, about 700 km to the west) run by West Australian Biogeochemistry Centre, The University of Western Australia, were very similar ($\delta^{18}O$ −4.75 ‰, $\delta^{2}H$ −24.2 ‰) to the interpolated values for Weebubbie Cave. This consistency in the values confirms that even though shorter, the local time series is representative of the local conditions at Weebubbie Cave.

In contrast to the weighted by volume mean annual precipitation, large volume precipitation events tend to have more negative stable isotope compositions than mean weighted by volume precipitation (Dogramaci et al., 2012; Skrzypek et al., 2019). Also at Maryland Loo, monthly mean values for the wet season, which are dominated by large precipitation events, are much lower than weighed by volume mean precipitation. For example, $\delta^{18}O$ −7.24 ‰ and $\delta^{2}H$ −41.1 ‰ were observed for June 2015 (47 mm), and $\delta^{18}O$ −8.32 ‰ and $\delta^{2}H$ −47.1 ‰ for July 2015 (51 mm). A single, one-day 91 mm storm on 10/02/2017 had even lower values at $\delta^{18}O$ −8.86 ‰ and $\delta^{2}H$ −57.3 ‰ (Table S2).

The mean stable isotope composition of shallow ocean water has significantly more positive δ-values compared with rainfall and it is characterized by low spatial variability (LeGrande and Schmidt, 2006). In this study, we used local $\delta^{18}O$ 0.72 ‰ and $\delta^{2}H$ 2.63 ‰ for the Southern Ocean coast, calculating means from the data set collected by RV Falkor (The Schmidt Ocean Institute) during a hydrochemical survey on the continental shelf at Bremer Bay (34° 30″ S 119° 30″ E) (Trotter et al., 2020).

The stable isotope composition of the potential end-members listed above, cave waters, and precipitation allowed construction of four linear regression models (Fig. 5AB). LMWL ($\delta^{2}H = 7.25\ \delta^{18}O + 10.27$) was calculated for Maryland Loo using monthly means and the PWLSR method (Hughes and Crawford, 2012). The local cave water line (LCWL) was calculated using all cave water results ($\delta^{2}H = 5.40\ \delta^{18}O - 7.32$). Mixing Line 1 was calculated using two end-members: mean precipitation and ocean water. Mixing Line 2 was calculated using also two end-members: large volume precipitation and ocean water (Fig. 5 AB). LCWL is significantly different from potential mixing lines; therefore, it is likely reflecting the evaporation trend rather than mixing and can be similar to the Local Evaporation Line (LEL). LMWL, Mixing Line 1 and 2 create a mixing triangle that covers the whole range of potential stable isotope compositions which could result from mixing the three end-members considered (a, b, c and grey triangle on Fig. 5AB).

The mean cave water $\delta^{18}O$ (−4.34 ± 0.09 ‰) is slightly more positive and $\delta^{2}H$ (−31.1 ± 2.2 ‰) more negative compared with the weighted by volume mean local meteoric precipitation. The point representing Weebubbie Cave water is located far to the right of the LMWL and outside the mixing triangle. The $\delta^{2}H$ and $\delta^{18}O$ values for Weebubbie Cave water are below the hypothetical mixing lines between local ocean water and mean precipitation (Mix 1) or large volume precipitation (Mix 2) (Fig. 5AB). These stable hydrogen and oxygen isotope signatures suggest that contribution of the ocean water is unlikely despite the cave location being only 11 km from the Southern Ocean coastline, the cave depth down to ~40 m below sea level, and very low mean annual precipitation of 275 mm. This may suggest a large continental groundwater discharge to the Southern Ocean despite the arid climate of this part of the continent (Haynes et al., 2007; Lamontagne et al., 2015; Stewart et al., 2015).

More negative than in precipitation, $\delta^{2}H$ signatures of the cave water (signature is located below LMWL, Fig. 5) and the mean d-excess of ~3.6 ‰ (defined as $d = \delta^{2}H - 8 \times \delta^{18}O$) suggest the primary origin of the cave water is from partially evaporated, infrequent, large volume precipitation events with more negative $\delta^{18}O$ and $\delta^{2}H$ values (Fig. 5) rather than direct recharge from mean annual precipitation (Skrzypek et al., 2015). This conclusion could be confirmed further by calculation of the crossing point between LMWL and LCWL ($\delta^{18}O$ −8.88 ‰ and $\delta^{2}H$ −55.3 ‰), which defines the initial composition of water (Fellman et al., 2011). The value of the crossing point (point a on Fig. 5A) is exactly in the range observed for large precipitation events at Maryland Loo and almost exactly the same as the largest observed precipitation event of 91 mm ($\delta^{18}O$ −8.86 ‰ and $\delta^{2}H$ −57.3 ‰), suggesting that the value at the LMWL-LCWL crossing point is the same as the initial stable isotope composition of water contributing to the cave. Hence, the LCWL can be considered the LEL, reflecting the progress of evaporation of water before recharging to the caves or from the caves directly. Using the Craig-Gordon model, Stable Isotope Hydrocalculator (Skrzypek et al., 2015) and assuming the same mean temperature as the cave water (18.6 °C), expected relative humidity during evaporation 60–85 %, and initial water composition as for the calculated crossing point (−8.88 ‰ and −55.3 ‰), the cave water in Weebubbie Cave (−4.34 ‰ and −31.1 ‰) lost to evaporation is ~16 to 20 % of the initial volume delivered from large precipitation events. This range of evaporative losses is similar to those estimated for groundwater in other semi-arid regions in Western Australia (Skrzypek et al., 2019; Tugwell-Wootton et al., 2020).

High spatial homogeneity of cave water, as found in Weebubbie, was also observed in other caves in the region and reflected in low standard deviations: Murra-El-Elevyn ($\delta^{18}O$ −3.85 ‰, SD 0.07 ‰ $\delta^{2}H$ −28.7 ‰, SD 0.5 ‰, n = 14 in October 2013) and Cocklebiddy ($\delta^{18}O$ –4.85 ‰, SD 0.05 ‰ $\delta^{2}H$ −32.9 ‰, SD 1.7 ‰, n = 14 in January 2012). However, mean values were significantly different, likely reflecting the difference in evaporative losses between the caves due to different geomorphology and local recharge conditions. Contrastingly, the cave water in Tommy Graham's, where a halocline was reported at 20 m (Contos et al., 2001), displayed large spatial stable isotope heterogeneity ($\delta^{18}O$ -3.12 ‰, SD 0.40 ‰ $\delta^{2}H$ −23.4 ‰, SD 3.5 ‰, n = 6 in October 2013), associated with two major water masses with very different composition (Fig. 5B). Among the four compared caves, the highest $\delta^{18}O$ and $\delta^{2}H$ were in Tommy Graham's, and can be attributed to the highest evaporative losses. The greater losses may be associated with the higher water temperature in this cave (23.4 °C in 2009) which is about >4 °C above the local mean atmospheric temperature (www.bom.gov.au, site 011003, the period 1930–2010). However, the input of ocean water cannot be ruled out in Tommy Graham's Cave at this stage of our investigation.

4.3. Stable carbon isotope composition and salinity of cave water

The stable carbon isotope composition of dissolved inorganic carbon across Weebubbie Cave was also very homogenous, with $\delta^{13}C$ (DIC) varying in a very narrow range between 0.2 and 0.5 ‰. These $\delta^{13}C$(DIC) values are significantly above the range expected for surface freshwater (>−10 ‰, e.g. Siebers et al., 2020). They are also below the values observed for the Southern Ocean (1.2–1.5 ‰ at 5 m depth in Bremer Bay in 2020, Trotter et al., 2020) implying a lack of a direct exchange with ocean water. The $\delta^{13}C$(DIC) values can be dominated by the dissolution of the marine carbonates that form the Nullarbor Platform and is not indicative of a potential geothermal or juvenile CO_2 input, which is usually characterised by very low $\delta^{13}C$ values (Bergfeld et al., 2001; Dogramaci and Skrzypek, 2015b; Janik and McLaren, 2010; Mather et al., 2018).

The salinity of water in Weebubbie Cave (23.3 mS/cm) was also uniform (Contos et al., 2001; Holmes et al., 2001), with total dissolved solids below half of what is typical for the ocean water, (~35 g/L). In contrast to water, which according to the stable isotope evidence originates from precipitation, the major ion ratios suggest that some solutes have ocean origin, e.g. Cl/SO_4 ratio 0.11 (ratio as meq/L). This Cl/SO_4 ratio is in the range of precipitation typical for coastal locations and seawater (0.10–0.15 ratio as meq/L, Dogramaci and Skrzypek, 2015a; Hingston and Gailitis, 1976). However, bicarbonates concentration was relatively low (89 mg/L) and contrastingly nitrates extremely high (100 mg/L) and far above values expected for ocean water (Contos et al., 2001; Price et al., 2012). This hydrochemical composition also does not imply direct interaction with ocean water. High groundwater and cave water salinity could be the result of sea salt transported with precipitation or sea spray, accumulated and recycled over millennia as described in other arid regions of Western Australia (Skrzypek et al., 2013, 2016).

5. Conclusion

Previous research has identified thermoclines in Nullarbor caves but resulting from the ingress of rainwater. In this study, we propose an entirely different thermal phenomenon. The hydrochemical and stable isotope analyses suggest that thermal irregularity at the Air Dome of Weebubbie Cave is rather associated with heat transfer than the inflow of warm water. The stable hydrogen and oxygen isotope compositions also confirm that the cave water originates from partially evaporated, modern, local, large precipitation events. Despite the relatively high salinity of water (23.3 mS/cm) and the location of the flooded cave sections below sea level, direct ocean water contribution to the cave system seems unlikely. The stable isotope composition of the cave water adds new perspectives on the discharge-recharge cycle, suggesting that only very large, infrequent precipitation events with very negative δ-values are contributing to the water in Weebubbie Cave. Further thermal and hydrochemical research in Weebubbie and other flooded Nullarbor caves is needed to confirm the origin of the heat transfer and understand processes contributing to observed water hydrochemistry. Such research may help verify speleogenesis hypotheses of large Nullarbor caves (which are the largest in Australia), better understand discharge-recharge in karstic aquifers, and to recognize the significance of the hydrochemistry of brackish waters for unique underground ecosystems.

CRediT authorship contribution statement

Peter Buzzacott: Conceptualization, Formal analysis, Investigation, Methodology, Writing - original draft, Visualization, Writing - review & editing. **Grzegorz Skrzypek:** Conceptualization, Formal analysis, Investigation, Methodology, Writing - original draft, Visualization, Writing - review & editing.

Declaration of Competing Interest

The authors declare that they have no known competing financial interests or personal relationships that could have appeared to influence the work reported in this paper.

Acknowledgments

This study was funded, in part, by two research grants from the Australian Speleological Federation. The Department of Regional Development and Lands permitted access to Weebubbie Cave. All divers were current members of the Cave Divers Association of Australia and their assistance is gratefully acknowledged. In particular, Andrew Robertson is thanked for his assistance both above and below the water. The authors also thank Hisayo Thornton for modifying the map of Weebubbie Cave included in this paper as Fig. 2; the original was drawn by Ian Lewis, who was also kind enough to comment on an early draft of this manuscript. Thanks to Will Carmody, Maryland Loo station owner for the long-term rain samples collection and Sean Elliott, Andrew Fleming, and Damian Wright for providing the photographs used in Fig. 1. The authors thank Dr Johannes Barth and two other reviewers for their comments and suggestions.

Appendix A. Supplementary data

Supplementary material related to this article can be found, in the online version, at doi:https://doi.org/10.1016/j.ejrh.2021.100793.

References

Awaleh, M.O., et al., 2020. Hydrochemistry and multi-isotope study of the waters from Hanlé-Gaggadé grabens (Republic of Djibouti, East African Rift System): a low-enthalpy geothermal resource from A transboundary aquifer. Geothermics 86. https://doi.org/10.1016/j.geothermics.2020.101805.

Bergfeld, D., Goff, F., Janik, C.J., 2001. Elevated carbon dioxide flux at the Dixie Valley geothermal field, Nevada; Relations between surface phenomena and the geothermal reservoir. Chem. Geol. 177 (1–2), 43–66. https://doi.org/10.1016/S0009-2541(00)00381-8.

Bicanic, J., 2017. Cave diving in Weebubbie Cave, Australia. Scuba Life (110), 66–70.

Boulton, A.J., Humphreys, W.F., Eberhard, S.M., 2003. Imperilled subsurface waters in Australia: biodiversity, threatening processes and conservation. Aquat. Ecosyst. Health Manage. 6 (1), 41–54. https://doi.org/10.1080/14634980301475.

Bowen, G.J., Revenaugh, J., 2003. Interpolating the isotopic composition of modern meteoric precipitation. Water Resour. Res. 39 (10), SWC91–SWC913. https://doi.org/10.1029/2003WR002086.

Bureau of Meteorology, 2013. Climate Statistics for Australian Locations - Eucla. Australian Government.

Burnside, N.M., Banks, D., Boyce, A.J., Athresh, A., 2016. Hydrochemistry and stable isotopes as tools for understanding the sustainability of minewater geothermal energy production from a 'standing column' heat pump system: Markham Colliery, Bolsover, Derbyshire, UK. Int. J. Coal Geol. 165, 223–230. https://doi.org/10.1016/j.coal.2016.08.021.

Buzzacott, P., 2011a. Murra-El-Elevyn water temperature. Caves Australia (187), 17–19.

Buzzacott, P., 2011b. Tommy Graham's Cave temperature study. Caves Australia (184), 18–19.

Calligaris, C., Mezga, K., Slejko, F.F., Urbanc, J., Zini, L., 2018. Groundwater characterization by means of conservative ($\delta^{18}O$ and $\delta^{2}H$) and non-conservative ($^{87}Sr/^{86}Sr$) isotopic values: the classical karst region aquifer case (Italy–Slovenia). Geosciences (Switzerland) 8 (9). https://doi.org/10.3390/geosciences8090321.

Contos, A.K., James, J.M., Heywood, B., Pitt, K., Rogers, P., 2001. Morphoanalysis of bacterially precipitated subaqueous calcium carbonate from Weebubbie Cave, Australia. Geomicrobiol. J. 18, 331–343.

Coplen, T., 1996. New guidelines for reporting stable hydrogen, carbon, and oxygen isotope-ratio data. Geochimica et Cosmochimica Acta 60, 3359.

Dogramaci, S., Skrzypek, G., 2015a. Unravelling sources of solutes in groundwater of an ancient landscape in NW Australia using stable Sr, H and O isotopes. Chem. Geol. 393-394, 67–78. https://doi.org/10.1016/j.chemgeo.2014.11.021.

Dogramaci, S., Skrzypek, G., 2015b. Unravelling sources of solutes in groundwater of an ancient landscape in NW Australia using stable Sr, H and O isotopes. Chem. Geol. 393-4, 67–78.

Dogramaci, S., Skrzypek, G., Dodson, W., Grierson, P., 2012. Stable isotope and hydrochemical evolution of groundwater in the semi-arid Hamersley Basin of subtropical northwest Australia. J. Hydrogeol. 475, 281–293.

Emmett, A.J., Telfer, A.L., 1994. Influence of karst hydrology on water quality management in southeast South Australia. Environ. Geol. 23 (2), 149–155. https://doi.org/10.1007/bf00766988.

Fellman, J.B., Dogramaci, S., Skrzypek, G., Dodson, W., Grierson, P.F., 2011. Hydrologic control of dissolved organic matter biogeochemistry in pools of a subtropical dryland river. Water Resour. Res. 47 https://doi.org/10.1029/2010WR010275.

Fusari, A., et al., 2017. Circulation path of thermal waters within the Laga foredeep basin inferred from chemical and isotopic ($\delta^{18}O$, δD, 3H, $^{87}Sr/^{86}Sr$) data. Appl. Geochem. 78, 23–34. https://doi.org/10.1016/j.apgeochem.2016.11.021.

Gee, G.W., Hillel, D., 1988. Groundwater recharge in arid regions: review and critique of estimation methods. Hydrol. Processes 2 (3), 255–266. https://doi.org/10.1002/hyp.3360020306.

Gibson, L., Humphreys, W.F., Harvey, M., Hyder, B., Winzer, A., 2019. Shedding light on the hidden world of subterranean fauna: a transdisciplinary research approach. Sci. Total Environ. 684, 381–389. https://doi.org/10.1016/j.scitotenv.2019.05.316.

Gillieson, D., Spate, A., 1992. The Nullarbor Karst. In: Gillieson, D. (Ed.), Geology, Climate, Hydrology and Karst Formation: IGCP Project 299, Field Symposium, Vol. 4. Department of Georgraphy and Oceanography, Australian Defence Academy Special Publication, Canberra, pp. 65–99.

Gregoric, A., Vaupotic, J., Sebela, S., 2014. The role of cave ventilation in governing cave air temperature and radon levels (Postojna Cave, Slovenia). Int. J. Climatol. 34 (5), 1488–1500.

Gröning, M., 2011. Improved water $\delta^{2}H$ and $\delta^{18}O$ calibration and calculation of measurement uncertainty using a simple software tool. Rapid Commun. Mass Spectrom. 25 (19), 2711–2720. https://doi.org/10.1002/rcm.5074.

Gröning, M., et al., 2012. A simple rain collector preventing water re-evaporation dedicated for $\delta^{18}O$ and $\delta^{2}H$ analysis of cumulative precipitation samples. J. Hydrol. 448-449, 195–200. https://doi.org/10.1016/j.jhydrol.2012.04.041.

Haynes, D., Gell, P., Tibby, J., Hancock, G., Goonan, P., 2007. Against the tide: the freshening of naturally saline coastal lakes, southeastern South Australia. Hydrobiologia 591 (1), 165–183. https://doi.org/10.1007/s10750-007-0802-7.

Herczeg, A.L., Leaney, F.W., 2011. Review: environmental tracers in arid-zone hydrology. Hydrogeol. J. 19 (1), 17–29. https://doi.org/10.1007/s10040-010-0652-7.

Hingston, F.J., Gailitis, V., 1976. Geographic variation of salt precipitated over Western-Australia. Aust. J. Soil Res. 14 (3), 319–335. https://doi.org/10.1071/sr9760319.

Holmes, A.J., et al., 2001. Phylogenetic structure of unusual aquatic microbial formations in Nullarbor Caves, Australia. Environ. Microbiol. 3 (4), 256–264.

Hughes, C., Crawford, J., 2012. A new precipitation weighted method for determining the meteoric water line. J. Hydrol. 464–465, 344–351.

James, J.M., Contos, A.K., Barnes, C.M., White, W.B., Culver, D.C., 2012. Nullarbor Caves, Australia, Encyclopedia of Caves (Second Edition). Academic Press, Amsterdam, pp. 568–576. https://doi.org/10.1016/B978-0-12-383832-2.00084-0.

Janik, C.J., McLaren, M.K., 2010. Seismicity and fluid geochemistry at Lassen Volcanic National Park, California: evidence for two circulation cells in the hydrothermal system. J. Volcanol. Geotherm. Res. 189 (3–4), 257–277. https://doi.org/10.1016/j.jvolgeores.2009.11.014.

Jasechko, S., Wassenaar, L.I., Mayer, B., 2017. Isotopic evidence for widepread cold-season-biased groundwater recharge and young streamflow across central Canada. Hydrol. Processes 31, 2196–2209.

Kaufmann, G., Gabrovsek, F., Romanov, D., 2014. Deep conduit flow in larst aquifers revisited. Water Resour. Res. 50 (6), 4821–4836.

Lachniet, M.S., 2009. Climatic and environmental controls on speleothem oxygen-isotope values. Quat. Sci. Rev. 28 (5–6), 412–432. https://doi.org/10.1016/j.quascirev.2008.10.021.

Lamontagne, S., Taylor, A.R., Herpich, D., Hancock, G.J., 2015. Submarine groundwater discharge from the South Australian Limestone Coast region estimated using radium and salinity. J. Environ. Radioact. 140, 30–41. https://doi.org/10.1016/j.jenvrad.2014.10.013.

LeGrande, A.N., Schmidt, G.A., 2006. Global gridded data set of the oxygen isotopic composition in seawater. Geophys. Res. Lett. 33 (12) https://doi.org/10.1029/2006GL026011.

Lewis, I.D., 1979. The Nullarbor Plain and the world's longest cave dive. Caving Int. (3), 3–10.

Lewis, I.D., 2019. South Australian geology and the State Heritage Register: an example of geoconservation of the Naracoorte Caves complex and karst environment. Aust. J. Earth Sci. 66 (6), 785–792. https://doi.org/10.1080/08120099.2019.1608300.

Lowry, D.C., Jennings, J.N., 1974. The Nullarbor Karst. Australia. Zeitschrift fùr Geomorphologie 18, 35–81.

Markowska, M., et al., 2016. Semi-arid zone caves: evaporation and hydrological controls on δ18O drip water composition and implications for speleothem paleoclimate reconstructions. Quat. Sci. Rev. 131, 285–301. https://doi.org/10.1016/j.quascirev.2015.10.024.

Mather, C.C., Skrzypek, G., Dogramaci, S., Grierson, P.E., 2018. Paleoenvironmental and paleohydrochemical conditions of dolomite formation within a saline wetland in arid northwest Australia. Quat. Sci. Rev. 185, 172–188.

McKnight, T.L., Hess, D., 2000. Climate Zones and Types: Dry Climates (Zone B). Physical Geography: a Landscape Appreciation. Prentice Hall, Upper Saddle River, NJ.

Paul, D.B., Skrzypek, G., 2007. Assessment of carbonate-phosphoric acid analytical technique performed using GasBench II in continuous flow isotope ratio mass spectrometry. Int. J. Mass Spectrometry 262, 180–186.

Poulter, N., 1987. The cleanup of Weebubbie Cave. Helictite 25 (2), 43–46.
Price, R.M., Skrzypek, G., Grierson, P.F., Swart, P.K., Fourqurean, J.W., 2012. The use of stable isotopes of oxygen and hydrogen to identify water sources in two hypersaline estuaries with different hydrologic regimes. Mar. Freshwater Res. 63 (11), 952–966. https://doi.org/10.1071/MF12042.
Rau, G.C., et al., 2015. Controls on cave drip water temperature and implications for speleothem-based paleoclimate reconstructions. Quat. Sci. Rev. 127, 19–36. https://doi.org/10.1016/j.quascirev.2015.03.026.
Richards, A.M., 1971. An ecological study of the cavericolus fauna of the Nullarbor Plain, Southern Australia. J. Zool. Lond. 164, 1–60.
Schwarz, K., Barth, J.A.C., Postigo-Rebollo, C., Grathwohl, P., 2009. Mixing and transport of water in a karst catchment: a case study from precipitation via seepage to the spring. Hydrol. Earth Syst. Sci. 13 (3), 285–292. https://doi.org/10.5194/hess-13-285-2009.
Siebers, A.R., Pettit, N.E., Skrzypek, G., Dogramaci, S., Grierson, P.F., 2020. Diel cycles of $\delta^{13}C_{DIC}$ and ecosystem metabolism in ephemeral dryland streams. Aquat. Sci. 82 (2) https://doi.org/10.1007/s00027-020-0708-2.
Skrzypek, G., 2013. Normalization procedures and reference material selection in stable HCNOS isotope analyses – an overview. Anal. Bioanal.Chem. 405, 2815–2823.
Skrzypek, G., Ford, D., 2014. Stable isotope analyses of saline water samples on a cavity ring-down spectroscopy instrument. Environ. Sci. Technol. 48, 2827–2834.
Skrzypek, G., Dogramaci, S., Grierson, P.F., 2013. Geochemical and hydrological processes controlling groundwater salinity of a large inland wetland of northwest Australia. Chem. Geol. 357, 164–177. https://doi.org/10.1016/j.chemgeo.2013.08.035.
Skrzypek, G., et al., 2015. Estimation of evaporative loss based on the stable isotope composition of water using Hydrocalculator. J. Hydrol. 523, 781–789.
Skrzypek, G., Dogramaci, S., Rouillard, A., Grierson, P.F., 2016. Groundwater seepage controls salinity in a hydrologically terminal basin of semi-arid northwest Australia. J. Hydrol. 542, 627–636. https://doi.org/10.1016/j.jhydrol.2016.09.033.
Skrzypek, G., Dogramaci, S., Page, G.F.M., Rouillard, A., Grierson, P.F., 2019. Unique stable isotope signatures of large cyclonic events as a tracer of soil moisture dynamics in the semiarid subtropics. J. Hydrol. 578 https://doi.org/10.1016/j.jhydrol.2019.124124.
Stewart, B.T., Santos, I.R., Tait, D., Macklin, P.A., Maher, D.T., 2015. Submarine groundwater discharge and associated fluxes of alkalinity and dissolved carbon into Moreton Bay (Australia) estimated via radium isotopes. Mar. Chem. 174, 1–12. https://doi.org/10.1016/j.marchem.2015.03.019.
Talà, A., et al., 2021. Chemotrophic profiling of prokaryotic communities thriving on organic and mineral nutrients in a submerged coastal cave. Sci. Total Environ. 755, 142514 https://doi.org/10.1016/j.scitotenv.2020.142514.
Tetu, S.G., et al., 2013. Life in the dark: metagenomic evidence that a microbial slime community is driven by inorganic nitrogen metabolism. ISME J. 7 (6), 1227–1236. https://doi.org/10.1038/ismej.2013.14.
Trotter, J., et al., 2020. Cruise FK200126 on RV Falkor. UWA. https://doi.org/10.7284/908818.
Tugwell-Wootton, T., Skrzypek, G., Dogramaci, S., McCallum, J., Grierson, P.F., 2020. Soil moisture evaporative losses in response to wet-dry cycles in a semiarid climate. J. Hydrol. 590 https://doi.org/10.1016/j.jhydrol.2020.125533.
Van Geldern, R., Barth, J.A.C., 2012. Optimization of instrument setup and post-run corrections for oxygen and hydrogen stable isotope measurements of water by isotope ratio infrared spectroscopy (IRIS). Limnol. Oceanogr. Methods 10, 1024–1036.
Vysoká, H., et al., 2019. Hydrogeology of the deepest underwater cave in the world: Hranice Abyss, Czechia. Hydrogeol. J. 27 (7), 2325–2345. https://doi.org/10.1007/s10040-019-01999-w.
Webb, J.A., James, J.M., 2006. Karst evolution of the Nullarbor Plain, Australia. In: Harmon, R.S., Wicks, C. (Eds.), Perspectives on Karst Geomorphology, Hydrology, and Geochemistry - A Tribute Volume to Derek C. Ford and William B. White: Geological Society of America, Special Paper 404. Geological Society of America, pp. 65–78.
Webb, J.A., White, S., 2013. Karst in deserts. In: Shroder, J.F. (Ed.), Treatise on Geomorphology. Academic Press, San Diego, pp. 397–406. https://doi.org/10.1016/B978-0-12-374739-6.00138-X.
White, N.E., et al., 2020. Detection of the rare Australian endemic blind cave eel (Ophisternon candidum) with environmental DNA: implications for threatened species management in subterranean environments. Hydrobiologia 847 (15), 3201–3211. https://doi.org/10.1007/s10750-020-04304-z.
Wilk, K., 2006. Sensus Ultra Developer's Guide. ReefNet, Ontario, p. 16.
Williams, T.M., Amatya, D.M., Hitchcock, D.R., Edwards, A.E., 2014. Streamflow and nutrients from a karst watershed with a downstream embayment: Chapel branch creek. J. Hydrol. Eng. 19 (2), 428–438. https://doi.org/10.1061/(asce)he.1943-5584.0000794.
Zhang, P., et al., 2008. A test of climate, sun, and culture relationships from an 1810-year Chinese cave record. Science 322 (5903), 940–942. https://doi.org/10.1126/science.1163965.